Reinvestigation of the Shape and State of Hydration of the Skeletal Myosin Subfragment 1 Monomer in Solution[†]

Manuel Garrigos, Jean E. Morel,* and José Garcia de la Torre

ABSTRACT: Hydrodynamic calculations lead to the conclusion that chymotryptic (or ethylenediaminetetraacetic acid) myosin S1 in solution (hydrated), at 1–5 °C, can be modeled as a prolate ellipsoid, with an axial ratio lying between $p = 1.0$ and 2.5 (major axis between 100.5 Å, for $p = 1.0$, and 162.5 Å, for $p = 2.5$). The degree of hydration is considerable (1.24 g/g for $p = 2.5$ and 2.02 g/g for $p = 1.0$). The dehydrated myosin head is pear-shaped under the electron microscope, and its narrowest part is located near the junction with the tail [Elliott, A., & Offer, G. (1978) J. Mol. Biol. 123, 505–519]. Mendelson & Kretzschmar [Mendelson, R. A., & Kretzschmar, K. M. (1980) Biochemistry 19, 4103–4108] have shown that the pear-shaped molecule does not predict the experimental X-ray scattering curve. Nor is this model able to predict the hydrodynamic values. The three-dimensional model for S1 used by Mendelson and Kretzschmar gives a rather good fit to the experimental X-ray scattering curve, but it does not predict the hydrodynamic values. In order to try to reconcile the three models and to fit the X-ray scattering curve and the hydrodynamic data, we suggest that, in solution, the S1 monomer has the shape of a prolate ellipsoid and that an inclusion of bound water exists at one extremity of the protein. The rest of bound water surrounds the protein. As first approximation, the dry protein and the hole are assumed to have the same shape as the hydrated molecule (prolate ellipsoid; p). Moreover, the long axis of the hole is assumed to lie along the long axis of the protein. The calculation of the radius of gyration and the intensity of X-ray scattering for such a model and the comparison with the available data lead to the conclusion that the S1 monomer in solution can be modeled as a prolate ellipsoid of moderate axial ratio $p = 2.3$ (major axis 156.5 Å; minor axis 68.0 Å), with an unusually high degree of hydration (1.37 g/g). The dry protein has a major axis of 119.0 Å and a minor axis of 51.8 Å. The major axis of the hole is 78.0 Å and its minor axis, 34.0 Å. The hole is located at 20.5 Å from the center of the protein; i.e., it is completely at one extremity of the protein, although it includes the center of this protein. It is possible that there is an opening between the pocket of water and the outside. The presence of this large hole explains the pear shape of the dehydrated myosin head and maybe the complicated shape of dehydrated S1 attached to actin. The differences between the shape of the myosin heads and that of S1 in solution cannot be accounted for by a noticeable digestion. For instance, the maximum length of S1 found here (119 Å) and by Mendelson and Kretzschmar (120 Å) is well below the maximum length of the dehydrated head found by Elliott and Offer (190 Å). This difference is likely attributable to a stretching of the myosin head on dehydration. As concerns the dehydrated S1 attached to actin, the large hole in the ellipsoid could explain part of its shape, but it is probable that attachment to actin leads to further distortions.

Many physical properties of the skeletal myosin S1[1] in solution are known: molecular weight, intrinsic viscosity, rotary diffusion coefficient, radius of gyration, specific volume, and X-ray scattering curve. However, it has been recently shown, by means of analytical ultracentrifugation, that S1 exists in the form of a monomer–dimer mixture, in rapid reversible equilibrium (Morel & Garrigos, 1982). The equilibrium constant is sensitive to the composition of the buffer, the temperature, and the hydrostatic pressure. All the physical properties of S1, except the sedimentation coefficient, have been obtained at atmospheric pressure and in benign buffers [absence of Mg–(phosphate compounds), in particular]. Comparison of the results of the literature with the results of Morel & Garrigos (1982) indicates that these physical properties correspond to an almost pure monomer. This is very likely not true for the sedimentation coefficient. For the monomer, this coefficient, determined by Morel & Garrigos

(1982) at 20 °C, is 5.05 ± 0.05 S, which is significantly lower than the widely accepted value of 5.80 ± 0.10 S (Lowey et al., 1969; Yang & Wu, 1977). In light of the results obtained by Morel & Garrigos (1982), the value of 5.80 S would correspond to a monomer–dimer mixture, with a large proportion of dimer. This value of 5.80 S would be related to the fact that this coefficient was measured under a too high hydrostatic pressure (60 000 rpm, and most likely at a too high radial position in the cell). More recently, Mendelson & Kretzschmar (1980) have found a value of 6.00 ± 0.20 S, by performing their experiments at 4 °C and by making use of S1 concentrations up to 18 mg/mL. This recent value would correspond to a pure dimer (Morel & Garrigos, 1982) and would be explainable on the basis of a monomer–dimer equilibrium, which equilibrium constant increases by decreasing the temperature. Morel & Garrigos (1982) have also shown that the S1 monomer is very likely highly hydrated, in contrast with what was claimed by Elliott & Offer (1978). The conclusion of these authors was merely due to an erroneous choice for the molecular weight of the myosin heads (they took M_r 115 000 instead of M_r 130 000 for complete S1 (Mg·S1): Margossian et al., 1981).

[1] Abbreviations: S1, myosin subfragment 1; chymotryptic or EDTA S1, LC2-free S1 (LC2 = DTNB light chain); S1(A1), S1 containing only the A1 (or LC1) light chain; S1(A2), S1 containing only the A2 (or LC3) light chain; Mg·S1, complete S1, with all the light chains; rod, myosin tail; EDTA, ethylenediaminetetraacetic acid.

The case of physiological interest would have been that of Mg·S1, since this S1 species represents a complete S1, with all its light chains. Unfortunately, most of the physical properties of Mg·S1 are not known. Most data concern LC2-free S1 (chymotrypsin or EDTA·S1). In the particular case of Mendelson & Kretzschmar (1980), the S1 species is not entirely LC2 free, but the LC2 content is low, and we shall assume this "hybrid" S1 is close to LC2-free S1. We shall study below the case of LC2-free S1, and we shall assume that the absence of LC2 does not induce large distortions in the shape and degree of hydration of S1, as compared with that of Mg·S1. This assumption seems to be borne out by the preliminary observations of Mendelson & Kretzschmar (1980) and Mendelson & Giniger (1982) and the results of Mendelson (1982).

One of the main purposes of the present paper is to reconcile the prolate ellipsoid model, which is very helpful for interpreting hydrodynamic properties, with the pearlike shape observed in the dehydrated state (Elliott & Offer, 1978) and with the X-ray scattering curve obtained by Mendelson & Kretzschmar (1980).

Under Discussion, we consider the case where our value of 5.05 S for the sedimentation coefficient of the monomer at 20 °C might be erroneous. For that purpose, we take the usual value of 5.80 S, and we show that our conclusions remain valid, owing to the small difference between 5.05 and 5.80 S. We also discuss some recent models for S1, and we recall that it is extremely dangerous to compare data obtained by means of conventional electron microscopy and by means of X-ray scattering, for instance, especially in the case of S1, which is highly hydrated in solution.

In this paper, we study the case of a prolate ellipsoid, although we do not dismiss the oblate. However, we consider there are many convergent findings, indicating that S1 is elongated, not flattened. Anyhow, the calculations we present here could be easily redone for an oblate.

Methods

Dimensions and Degree of Hydration of a Prolate Ellipsoid. Yang & Wu (1977) have proposed an extremely attractive approach of the problem of the shape and degree of hydration of a protein in solution, by making use of three hydrodynamic parameters: the intrinsic viscosity $[\eta]$, the sedimentation coefficient s^0, and the rotary diffusion coefficient θ^0. As already pointed out by Morel & Garrigos (1982), S1 is an elongated protein [see also Squire (1981)], and we shall assume here that the hydrated S1 monomer can be modeled as a prolate ellipsoid of revolution of axial ratio p, major axis a, and minor axis b. The dimensions and degree of hydration of the ellipsoid can be calculated according to the following set of equations (valid at 4 °C) [see Yang (1961)]:

$$2a \text{ (Å)} = 1.47([\eta]M_r)^{1/3}(p^2/\nu)^{1/3} \tag{1a}$$

$$\delta \text{ (g/g)} = (1/V_1^0)([\eta]/\nu - \bar{V}) \tag{1b}$$

where $[\eta]$ is expressed in cubic centimeters per gram, M_r is the molecular weight, ν is Simha's coefficient, V_1^0 is the specific volume of bulk water (1.000 mL/g at 4 °C), and $\bar{V}$ is the apparent specific volume of the protein.

$$2a \text{ (Å)} = 0.0112[M_r(1 - \rho\bar{V})/s_{4,w}^0](Fp^{2/3}) \tag{2a}$$

$$\delta \text{ (g/g)} = (\bar{V}/V_1^0)[F^3(f//f_{min})^3 - 1] \tag{2b}$$

where $\rho = 1/V_1^0$. $s_{4,w}^0$ is expressed in svedbergs. $F = f_0/f$, where f is the frictional coefficient of the protein, given by $f = M_r(1 - \rho\bar{V})/(N_A s_{4,w}^0)$ (N_A = Avogadro's number; $s_{4,w}^0$ in seconds); f_0 is the frictional coefficient of the equivalent sphere,

with the same degree of hydration as the protein. F only depends on p and can be theoretically calculated (Yang, 1961). $f_{min} = 6\pi\eta(3M_r\bar{V}/4\pi N_A)^{1/3}$ (η = the viscosity of the solvent: 1.567 cP for water at 4 °C).

$$2a \text{ (Å)} = 200(10^{-5}\theta^0)^{-1/3}(Jp^2)^{1/3} \tag{3a}$$

$$\delta \text{ (g/g)} = (\bar{V}/V_1^0)[J(\xi/\xi_{min}) - 1] \tag{3b}$$

$J = \xi_0/\xi$, where ξ is the rotary frictional coefficient, given by $\xi = RT/(N_A\theta^0)$, ξ_0 is the frictional coefficient of the equivalent sphere, with the same degree of hydration as the protein. ξ_{min} is the frictional coefficient of the unhydrated sphere, given by $\xi_{min} = 6\eta(M_r\bar{V}/N_A)$ (Yang, 1961). As is the case for F, J can be theoretically calculated (Yang, 1961).

Note that eq 1–3a,b are independent of the distribution of bound water in the protein [J. T. Yang, personal communication; also Figure 20.1 in Tanford (1967)]. These equations are, therefore, valid for the following model, in which we shall consider the case of an inclusion of bound water at one extremity of the protein. In a more quantitative way, the presence of a hole in an ellipsoid must have a very small influence on the hydrodynamic properties. The only hydrodynamic effect one can foresee is translation–rotation coupling (for example, some spinning during sedimentation), caused by the noncoincidence of the particle's centers of mass, buoyancy, and resistance. Garcia Bernal & Garcia de la Torre (1980) have shown that the coupling effects are very small (say ~5%) for very asymmetric bodies, like bend rods and helices, and must be even smaller (say ~1%) for our hollowed ellipsoids, since they keep a high symmetry.

From the above sets of equations, it is possible to calculate $2a$ and δ as functions of p, by introducing the experimental values of M_r, $[\eta]$, $s_{4,w}^0$, and θ^0, which are all known for skeletal chymotryptic S1 monomer.

Radius of Gyration of a Prolate Ellipsoid with an Ellipsoidal Hole. We shall see below that it is possible to reconcile the hydrodynamic data, the X-ray scattering data, and the electron microscopy observations by assuming that there is an inclusion of bound water in S1. Note that Kretzschmar et al. (1978) have already suggested this possibility. However, they did not go deeper into this problem, since they did consider ellipsoids were probably inadequate models. We shall see, in the following, that an ellipsoid with a hole removes the inadequacy that these authors attributed to ellipsoids.

For the sake of simplicity, we shall assume that the inclusion has the shape of a prolate ellipsoid, with the same value of p as the whole hydrated molecule with a major axis α and minor axis β. Obviously, this is an oversimplification, and the included bound water might be dispersed in the form of small droplets at one extremity of the protein. However, in this case, no simple calculation is possible. The major axis of the pocket of bound water is assumed to lie on the major axis of the whole protein. Besides this inclusion, we shall assume that there is a peripheral layer of bound water around the molecule. Always for the sake of simplicity we shall assume that the dry protein lying under this peripheral layer is also a prolate ellipsoid of axial ratio p, major axis a^*, and minor axis b^*. This is another oversimplification, since it is probable that the peripheral layer of bound water is not so regularly arranged. All the characteristics of the model are recalled on Figure 1.

Since the degree of hydration δ is given for a given value of p (eq 1–3b) and since we have $a = pb$, $a^* = pb^*$, and $\alpha = p\beta$, we have the following relation between b, b^*, and β:

$$b^{*3} = b^3/(1 + \delta V_1/V_{sp}) + \beta^3 \tag{4}$$

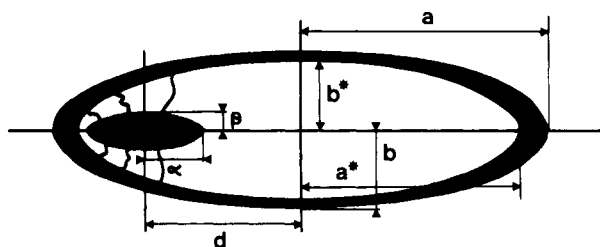V_1 is the specific volume of bound water and V_{sp} the specific

FIGURE 1: Shape of the S1 monomer in solution, according to our simplified model. The white zone represents the protein. The black zones represent bound water. The "winding" black lines represent bound water channels, by the intermediary of which bound water lying in the inclusion can leave the hole by dehydration. Obviously, these channels are not taken into account in our calculations. However, they might contribute to the X-scattering intensities, especially at high values of hR_G.

volume of the dehydrated protein. According to Tanford (1967), we have

$$\bar{V} = V_{sp} + \delta(V_1 - V_1^0) \tag{5}$$

from which we deduce $1 + \delta V_1/V_{sp} = (\bar{V} + \delta V_1^0)/V_{sp}$. Thus, eq 5 can also be written as

$$b^{*3} = b^3[V_{sp}/(\bar{V} + \delta V_1^0)] + \beta^3 \tag{6}$$

In this equation, $\bar{V}$ and V_1^0 are experimentally known. Morel & Garrigos (1982) have proposed the calculation of V_{sp}. Here, it is necessary to refine the calculation of the molecular weight for Mg·S1 and EDTA·S1, by taking into account the results of Margossian et al. (1981), corrected for a slight contamination by a S1 dimer (Morel & Garrigos, 1982). We found that the mean molecular weight of total S1 is 127 000. This value was obtained by averaging the molecular weight of Mg·S1 at $c = 0$ and that of EDTA·S1 at $c = 0$ (in this case, the value of the molecular weight of the LC2 light chain, 18 000, was added to the calculated value). Now, according to Elliott & Offer (1978), the volume of the dehydrated myosin head is 142 000 Å³. Therefore, we get $V_{sp} = 0.676$ mL/g. As already suggested by Morel & Garrigos (1982), we shall assume below that V_{sp} is the same for chymotryptic S1 as for a myosin head. To eq 6 we must add the following obvious condition:

$$d \leq a^* - \alpha \tag{7}$$

The radius of gyration of an ellipsoid having an ellipsoidal hole can be calculated from the particle's moments of inertia. These are in turn obtained from the formulas for the moments of inertia of solid ellipsoids by making use of Steiner's theorem. Thus, we arrive at the following analytical expression for the radius of gyration R_G:

$$R_G^2 = [(p^2 + 2)/5](b^{*5} - \beta^5)/(b^{*3} - \beta^3) - d^2\beta^3(b^{*3} - 2\beta^3)/(b^{*3} - \beta^3)^2 \tag{8}$$

where d is the center-to-center distance between the pocket of water and the protein (see Figure 1). For a given value of p, b and δ are given (see Tables III and IV). Moreover, b^* is related to b and β by means of eq 6. Thus, in our simplified model, R_G only depends on two parameters (d and β, for instance) for a given value of p. Note that eq 8 does not account for the fact that the specific volume of bound water is different from that of bulk water (see below), since "the low-angle X-ray scattering or neutron scattering does not distinguish water of hydration from free water" (Yang & Wu, 1977). Therefore, the measured value of R_G only corresponds to the dry protein, and eq 8 is directly comparable with the X-ray scattering experimental data.

Intensity of X-ray Scattering as a Function of the Angle of Observation. The calculation of the scattering form factor is done as follows. The white zone plus the inclusion of water (Figure 1) is filled with small spherical beads of radius σ, arranged in a closest packed configuration. Then, the beads whose centers are in the hole are removed. The scattering form factor, which is proportional to the deconvoluted scattering intensity, is calculated from the Debye equation for a model composed of N identical scatterers:

$$P(h) = P_s(h)(1/N^2)\sum_{i=1}^{N}\sum_{j=1}^{N} \sin (hr_{ij})/(hr_{ij}) \tag{9}$$

r_{ij} is the distance between the centers of the beads i and j. $P_s(h)$ is the form factor of the beads, given by

$$P_s(h) = [3(\sin u - u \cos u)/u^3]^2 \tag{10}$$

with $u = h\sigma$, where h is related to the angle of observation ψ and the wavelength λ of the X-rays by means of

$$h = (4\pi/\lambda) \sin (\psi/2) \tag{11}$$

Since $P(0) = 1$, $P(h)$ is directly comparable with the deconvoluted scattering intensity normalized so that $I(0) = 1$. In the numerical calculation of $P(h)$ from eq 9, σ was taken to be 2.3 Å, which is roughly $^1/_{11}$ of b^* (see below). Thus, N was close to about 1800 beads.

Other X-ray Scattering Calculations. In addition to the radius of gyration, there are other geometrical parameters of structural importance. The longest chord, l, is the longest intramolecular distance, and its value for a prolate ellipsoid is obviously $l = 2a^*$. The intramolecular distances, or chords (R), follow a probability distribution $p(R)$ with $p(R) = 0$ for $R > l$. R_G^2 is the second moment of $p(R)$, and its first moment is the mean chord $\bar{R}$. Finally, R_{max} is the most probable chord, defined as the value which maximizes $p(R)$. From the positions of the bead centers, the same computer code used for the calculation of $I(h)$ estimated $p(R)$ in the form of a histogram from which the values of R_{max} and $\bar{R}$ were obtained.

Results

Recall of Experimental Data. It is clear from eq 1–3a,b that, for each value of p, $2a$ and δ can be estimated when M_r, $[\eta]$, s^0, and θ^0 are experimentally known, which is the case for chymotryptic S1. In Table I, we recall the values of these parameters we have collected in the most recent literature. Note that, as pointed out by Yang & Wu (1977), there is a problem that concerns the rotary diffusion coefficient: the values at 4 and 20 °C do not fit after corrections for temperature and water viscosity. In sharp contrast, s^0 and $[\eta]$ are the same at 5 and 25 °C, in the limit of the experimental error, after the same corrections (Yang & Wu, 1977). We suggest, under Discussion, that this behavior might be due to variations in the shape and/or degree of hydration with temperature. In light of this difficulty, we shall take all the hydrodynamic values at 4 °C, in order to have a comparison with the data obtained by means of X-ray scattering, which have been obtained at 1 °C. As concerns the apparent specific volume $\bar{V}$, it is also a function of the temperature. According to Svedberg & Pedersen (1940), the apparent specific volume increases by 5×10^{-4} mL/(g·°C) and the specific volume $\bar{V}_4$ at 4 °C is related to the specific volume $\bar{V}_t$ at t by means of the formula

$$\bar{V}_4 = \bar{V}_t + 5 \times 10^{-4}(4 - t) \tag{12}$$

When the temperature at which the measurement of $\bar{V}$ has been done is given by the authors, we made the correction according to eq 12 (see Table I).

Possible Shapes and Degrees of Hydration of the S1 Monomer. Table II gives the values of the different shape factors,

Table I: Recall of Experimental Data Collected in the Literature[a]

	$s^0_{4,w}$ (S)	$10^{-5}\theta^0$ (s^{-1})	$[\eta]$ (cm^3/g)	M_r	R_G (Å)	$\bar{V}_4$ (mL/g)
min	3.25[b]	6.00[c]	5.90[f]	107 000[b]	32.0[k]	0.717[o] (26 °C)
mean	3.30[b]	6.90[c]	6.44[f]	110 300	33.0	0.728
max	3.35[b]	8.00[c]	7.10[f]	115 000[h]	35.0[l] (?)	0.740[k] (?)
other values		6.67[d] (20 °C)	6.40[g] (20 °C)	108 000[b]	32.8[h]	0.734[p] (?)
		7.58[e] (20 °C)		110 000[i]	32.4[m]	0.729[q] (?)
		10.22[e] (20 °C)		109 000[h]	32.7[n]	0.720[i]
				113 000[j]		0.730[m]

[a] Data at 1-5 °C, unless specified, for chymotryptic or EDTA S1. As concerns the sedimentation coefficient, the value obtained by Morel & Garrigos (1982) at 20 °C (5.05 ± 0.05 S) was corrected for water viscosity and specific volume ($\bar{V}_4$ was taken as 0.728 mL/g and $\bar{V}_{20}$ as 0.736 mL/g; see eq 12), in order to have the apparent value $s^0_{4,w}$. Note that this new value corresponds to the true value at 4 °C, since s^0 is the same at 5 and 25 °C, after corrections (Yang & Wu, 1977; also see Discussion). We have assumed the same error bar at 4 °C than at 20 °C (±0.05 S). The symbols "min" and "max", respectively, correspond to the lower and higher experimental values. θ^0 was calculated from the relation $\Phi = 1/_6\theta^0$, where Φ is the rotational correlation time. [b] Morel & Garrigos (1982). [c] Mendelson et al. (1973). [d] Kobayashi & Totsuka (1975). [e] Thomas et al. (1975). [f] J. T. Yang, personal communication. The values of the intrinsic viscosity were measured for both S1(A1) and S1(A2); the results were the same for both isoenzymes, in the limit of the experimental error; thus, it is reasonable to take, for LC2-free S1, which is a mixture of S1(A1) plus S1(A2), the same values as those for both isoenzymes. [g] Lowey et al. (1969).
[h] Mendelson & Kretzschmar (1980) (the value of 121 000 given by these authors was lowered by 6000, which represents about a 30-35% contamination by LC2). [i] Margossian et al. (1981). [j] Margossian & Stafford (1979). [k] Yang & Wu (1977). [l] Squire (1981).
[m] Kretzschmar et al. (1978). [n] Mendelson (1982). [o] Parrish & Mommaerts (1954) (the value of $\bar{V}$ is given for myosin and widely used for S1). [p] Garcia de la Torre & Bloomfield (1980). [q] Sakura & Reithel (1972). The symbol (?) indicates that the temperature is not specified by the authors.

Table II: Shape Factors, for Prolate Ellipsoids, as Functions of the Axial Ratio p [Deduced from Yang (1961)]

p	ν	$(p^2/\nu)^{1/3}$	$F = f_0/f$	$J = \xi_0/\xi$	$Fp^{2/3}$	$(Jp^2)^{1/3}$
1.0	2.50	0.737	1.000	1.000	1.000	1.000
1.5	2.63	0.949	0.985	0.820	1.291	1.226
2.0	2.91	1.112	0.958	0.665	1.521	1.385
2.3	3.12	1.190	0.938	0.581	1.631	1.446
2.5	3.26	1.242	0.925	0.525	1.704	1.486
3.0	3.68	1.347	0.899	0.427	1.871	1.567
3.5	4.14	1.436	0.875	0.355	2.017	1.632
4.0	4.66	1.509	0.846	0.295	2.132	1.676

deduced from the paper of Yang (1961). Tables III and IV give the values of $2a$ and δ, calculated from eq 1–3a,b and Tables I and II. The principle of our calculations is exactly that already described by Yang & Wu (1977). However, by introducing the error bars on the different experimentally known parameters, we were able to determine intersection zones for both $2a$ and δ. Both Tables III and IV show that p lies between 1.0 and 2.5. We conclude that the S1 monomer in solution can be modeled as a prolate ellipsoid of axial ratio ranging between $p = 1.0$ ($2a = 100.5$ Å; $\delta = 2.02$ g/g) and $p = 2.5$ ($2a = 162.5$ Å; $\delta = 1.24$ g/g). All these values are compatible with the reported values for the molecular weight and the three hydrodynamic parameters at 4 °C, in benign buffers. Note that the present procedure has the drawback to not allow us to give the exact value of p but only the range

of possible values of p. In the following section, we shall remove this ambiguity and we shall confirm that our hydrodynamic approach is suitable, which supports, in particular, the validity of the hydrodynamic equations 1–3a,b, irrespective of the distribution of bound water.

Most Probable Shape of the Hydrated S1 Monomer and the Shape of the Dehydrated Myosin Head. We have seen that all the values of p ranging between 1.0 and 2.5 are compatible with the hydrodynamic data and the molecular weight. This means that the S1 monomer in solution can be modeled as a prolate ellipsoid of moderate axial ratio. The calculation of R_G and $I(h)$ will allow us to refine the exact value of p and the other related parameters.

A case of major interest is that corresponding to the absence of a hole. Under these conditions, eq 8 reduces to

$$R_G = b^*[(p^2 + 2)/5]^{1/2} \qquad (13)$$

with b^* given by eq 6, which becomes here

$$b^* = b[V_{sp}/(\bar{V} + \delta V_1^0)]^{1/3} \qquad (14)$$

From eq 13 and 14, we see that the values of p ranging between 3.0 and 3.5 give values of R_G lying in the experimental error interval. We have calculated $I(h)$ according to eq 9 and to the procedure described above, for $p = 3.0$ and 3.5. In Figure 2, we have represented the experimental values of $I(h)$ and the two theoretical curves. We see that the fit is very poor. This behavior of the ellipsoids with no hole was already ob-

Table III: Values of the Long Axis $2a$, Calculated from eq 1–3a and by Introducing the Numerical Values Recalled in Tables I and II[a]

	$2a$ (Å)											
	$[\eta]$			s^0			θ^0					
p	min	mean	max	min	mean	max	min	mean	max	$2\bar{a}$ (Å)	Δ_a (Å)	$2a^+$ (Å)
1.0	94	97	101	93	103	112	100	105	110	102	100–101	100.5
1.5	121	125	131	120	133	145	122	129	135	129	120–131	125.5
2.0	142	146	152	142	157	171	138	145	152	149	142–152	147.0
2.3	152	156	163	154	167	183	144	152	159	158	154–159	156.5
2.5	159	163	171	162	174	191	148	156	163	164	162–163	162.5
3.0	172	176	185	177	191	211	156	164	172	177	–	–
3.5	183	187	198	187	207	226	163	171	179	188	–	–
4.0	193	197	207	198	219	239	167	175	181	197	–	–

[a] The symbol "mean" corresponds to the values of $2a$ deduced from the mean values of the experimental parameters (Table I). The symbols "min" and "max", respectively, correspond to the lower and higher values of $2a$, calculated from the values in Table I. $2\bar{a}$ represents the average of the three mean values. Δ_a is the intersection of the different error bars. $2a^+$ is the middle of the intersection and represents the most probable value of $2a$. The (–) indicates that there is no intersection of the error bars.

Table IV: Values of the Degree of Hydration δ, Calculated from eq 1-3b and by Making Use of the Same Procedure as That Presented in Table III[a]

	$[\eta]$			s^0			θ^0					
p	min	mean	max	min	mean	max	min	mean	max	$\bar{\delta}$ (g/g)	Δ_δ (g/g)	δ^+ (g/g)
1.0	1.62	1.85	2.12	1.65	2.34	3.70	1.92	2.49	3.10	2.22	1.92-2.12	2.02
1.5	1.50	1.72	1.98	1.55	2.21	3.51	1.44	1.92	2.41	1.94	1.55-1.98	1.77
2.0	1.28	1.49	1.72	1.37	1.96	3.15	1.03	1.41	1.82	1.61	1.37-1.72	1.54
2.3	1.15	1.35	1.36	1.24	1.83	2.92	0.81	1.15	1.51	1.44	1.24-1.51	1.37
2.5	1.07	1.25	1.46	1.16	1.73	2.78	0.66	0.97	1.31	1.31	1.16-1.31	1.24
3.0	0.86	1.04	1.21	1.00	1.50	2.50	0.40	0.64	0.91	1.06	–	–
3.5	0.68	0.83	1.00	0.86	1.31	2.24	0.21	0.42	0.64	0.85	–	–
4.0	0.53	0.65	0.81	0.71	1.12	1.96	0.05	0.22	0.41	0.66	–	–

[a] The different symbols have the same meaning as those used in Table III.
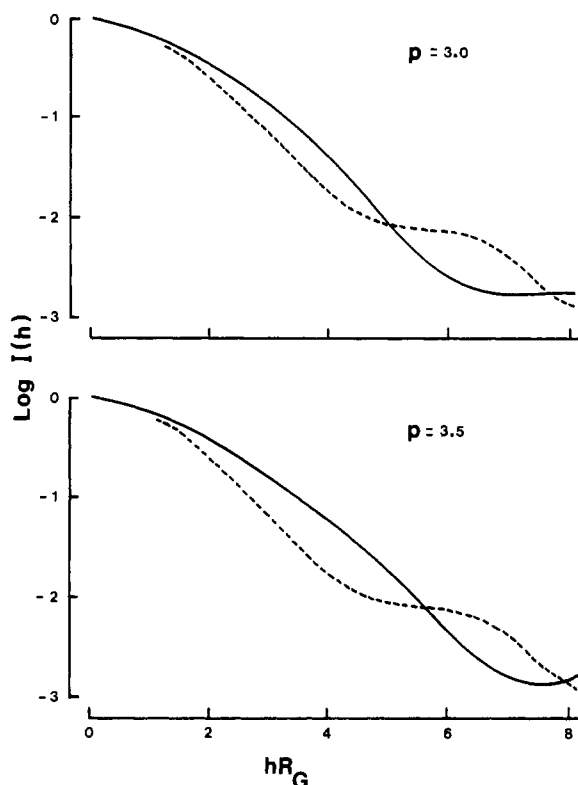
FIGURE 2: Values of $I(h)$ vs. the dimensionless parameter hR_G, for ellipsoids with no hole. The solid lines correspond to $p = 3.0$ and $p = 3.5$. The dashed lines represent the experimental deconvoluted intensities.

served by Mendelson & Kretzschmar (1980).

Let us now turn to the case where a hole exists in the ellipsoid. R_G is given by the general eq 8. In order to not complicate the problem, we shall assume that $R_G = 33.0$ Å (mean value; Table I) and we shall not consider the error bar. From eq 8, it is possible to calculate d as a function of b^*, β, and p, when R_G is fixed, which is the case here. We obtain

$$d^2 = [(b^{*3} - \beta^3)^2/\beta^3(b^{*3} - 2\beta^3)][(p^2 + 2) \times (b^{*5} - \beta^5)/5(b^{*3} - \beta^3) - R_G^2] \quad (15)$$

Since R_G is fixed (33.0 Å), as soon as p is given, d is a function of only one parameter, b^* or $a^* = pb^*$ for instance, since β is related to b^* by means of eq 6 and since b and δ are respectively given in Tables III and IV for each value of p. This equation will be used in the following. Note that eq 15 and inequality 7 are compatible only for $p < 3.2$ for our chosen value of R_G.

We have made many calculations of $I(h)$ for $p = 2.0$, 2.5, and 3.0 by varying the position and the dimensions of the hole.

Table V: Values of b^*, d, α, and β as Functions of a^*, for $p = 2.3$[a]

	a^* (Å)	b^* (Å)	d (Å)	α (Å)	β (Å)
(1)	58.0	25.2	0	35.0	15.2
(2)	58.5	25.4	11.3	36.3	15.8
(3)	59.0	25.7	18.6	37.7	16.4
(4)	59.5	25.9	20.5	39.0	17.0

[a] According to Table III, we have $b = 33.8$ Å. When a^* is varied, b^* varies according to the relation $a^* = 2.3b^*$. For each value of a^*, or b^*, β is deduced from eq 6 (with $\bar{V} = 0.728$ mL/g and $\delta = 1.37$ g/g; see Tables I and IV). Then, d is deduced from eq 15, since R_G is fixed at 33.0 Å. The higher value of a^* corresponds approximately to $d = a^* - \alpha$ (see inequality 7). The lower value of a^* corresponds to $d = 0$ (hole centered at the center of the molecule) and is obtained by solving the system of eq 6 and 8. The numbers on the left correspond to curves 1-4 in Figure 3.

We made the interesting observation that the scattering curve, for $hR_G < 4$, strongly depends on the value of p, but for a given value of p, it is very little sensitive to large changes in both the size and position of the hole. This circumstance could be used to estimate the best value of p, independently of the hole. We found a value of p extremely close to 2.3 in agreement with previous work (Kretzschmar et al., 1978). In the following we shall keep this value, which is compatible with the values obtained from the hydrodynamic approach. For $hR_G > 4$, there appeared a strong dependency on d and β. Thus, for $p = 2.3$, we varied a^*, and eq 15 gave a series of values of d and all the other characteristics of the hole, as functions of a^* (see Table V). The scattering curves corresponding to the four sets of values given in Table V are represented in Figure 3. The best fit seems to correspond to curve 4 in Figure 3 (see the values of the different characteristics of the hole in Table V). The values of the different parameters indicate that the inclusion of bound water represents ~0.20 g/g and that the surrounding layer represents ~1.20 g/g. The long axis of the hole represents $\sim66\%$ of the long axis of the dry protein, which is considerable and which explains that, by dehydration (electron microscopy), the myosin heads can adopt the shape of a pear.

Most Probable Values of the Molecular Weight, the Hydrodynamic Parameters, and Other Characteristics of the S1 Monomer in Solution. It is easy to show that the molecular weight of a hydrated prolate ellipsoid is given by

$$M_r = 2.52(pb^3)/(\bar{V} + \delta V_1^0) \quad (16)$$

where b is expressed in angstroms. On the other hand, according to eq 1b, we have

$$[\eta] = \nu(\bar{V} + \delta V_1^0) \quad (17)$$

The sedimentation coefficient $s_{4,w}^0$ (expressed in svedbergs) can be calculated from eq 6.62b in Tinoco et al. (1978):

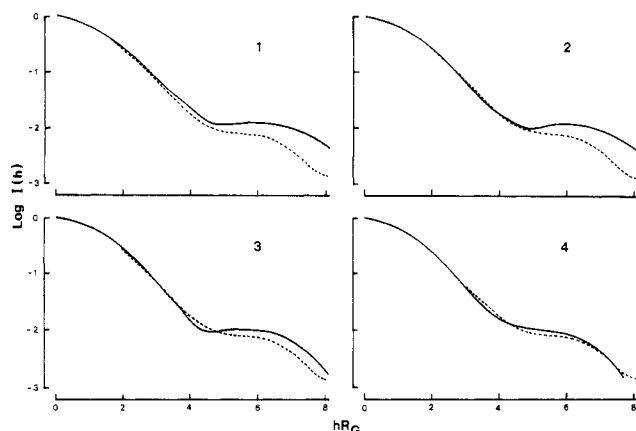$$s_{4,w}^0 = (M_r/1500)^{2/3}[\eta]^{-1/3}[(f_0/f)\nu^{1/3}](1 - \rho\bar{V}) \quad (18)$$

FIGURE 3: Values of $I(h)$ vs. hR_G, for $p = 2.3$ and for different values of a^*, given in Table V. The numbers 1, 2, 3, and 4 correspond to the numbers in Table V. The dashed lines have the same meaning as in Figure 2. For case 4 (and nearly case 3), we have $\alpha + d \sim a^*$, and the hole is completely at one extremity. Thus, the existence of "true channels" would be unnecessary because the protein must be very thin and surely hydrophylic at this extremity. We could even think there is an opening which communicates with the outside. Note that this extremity is certainly a "weak point". As far as, in the myosin molecule, the hole is located near the junction with the tail, we, *first*, obtain a very plausible explanation for the pearlike shape and, *second*, may explain why the action of proteolytic enzymes is so specific (absence of large amounts of digested material; see Conclusion). Such a structure may also explain the comma shape of S1 attached to actin (Figure 4).

Finally, the rotary diffusion coefficient at 4 °C is given by eq 3a, which can be written as

$$\theta^0 = 10^{11} J/(pb^3) \tag{19}$$

where b is once more expressed in angstroms.

The most probable values of b and δ, for $p = 2.3$, are given in Table III. After numerous calculations, we reached the conclusion that the best values of the molecular weight and the hydrodynamic parameters are obtained for $\bar{V}_4 = 0.735$ mL/g (i.e., $\bar{V}_{20} = 0.743$ mL/g). By making use of eq 16–19, we get $M_r = 107\,000$, $[\eta] = 6.57$ cm^3/g, $s^0_{4,w} = 3.34$ S ($s^0_{20,w} = 5.08$ S), $\theta^0 = 6.54 \times 10^5$ s^{-1} ($\Phi = 255$ ns) (at 4 °C), and $1/V_1 = 0.956$ g/mL (at 4 °C). All these values lie in the range of the experimental error (Table I), and they represent the most probable values for the chymotryptic or EDTA·S1 monomer in solution. Note that, if the molecular weight of the LC2 chain (18000) is added to 107000, we find 125000 for total S1 (Mg·S1), which is in good agreement with the value of 127000 given above.

As concerns the other characteristics of the protein, the problem might be difficult, owing to the fact that the calculations of Mendelson & Kretzschmar (1980) might not be valid when a hole exists (nonuniform electron density). Since X-ray scattering does not distinguish between bound and free water (Yang & Wu, 1977; Mendelson & Kretzschmar, 1980), we shall compare only the model for the dry protein with experiment. (i) The length of the long axis of the dry protein, we have found here, is $2a^* = 119$ Å, which practically coincides with the experimental value of 120 ± 10 Å found for the maximum chord (Mendelson & Kretzschmar, 1980). (ii) The volume of the dry protein (excluding the hole) is $(4\pi/3)(b^{*3} - \beta^3) = 120\,000$ Å^3, which does not exactly coincide with the experimental value of $151\,000 \pm 6000$ Å^3 (Mendelson & Kretzschmar, 1980). We note, however, that the experimental value was obtained for a not entirely LC2-free S1. Since the molecular weight of this species is $121\,000 \pm 5000$ and since the molecular weight of LC2-free S1 is 107000 (see above), the experimental value for LC2-free S1 would have

been $134\,000 \pm 11\,000$ Å^3, which is in reasonable agreement with 120000 Å^3. We also note that the hybrid S1 species studied by Mendelson & Kretzschmar (1980) has a volume higher than that obtained for a complete myosin head (142000 Å^3; see above). This discrepancy is very likely related to the nonuniform electron density, due to the hole. In this case, the calculation of Mendelson & Kretzschmar (1980) would be only an approximation, which might overestimate the dry volume. We have more confidence in the direct measurement made by Elliott & Offer (1978), which gives a volume of 120000 Å^3 for LC2-free S1, i.e., exactly the value we find here. The model's mean and most probable chords are found to be respectively $\bar{R} = 38$ Å and $R_{max} = 34$ Å, which compare well with the experimental results $\bar{R} = 41.5$ Å and $R_{max} = 36$ Å (Mendelson & Kretzschmar, 1980). These differences (2–4 Å) seem reasonable if one considers the limited resolution of the model that is determined by the finite separation between the centers of neighboring beads ($2\sigma = 4.6$ Å). The resolution could be improved by decreasing σ, but then the calculation of $I(h)$ would become unpractical, since computer time grows as σ^{-6}. We also note that the above differences are of the same order as those found for R_G, $\bar{R}$, and R_{max} in the case of electron microscopy reconstruction scaled to match the experimental volume (Mendelson, 1982).

Discussion

Consequences of the Choice of the Value of s^0 on the Characteristics of the Model. Although Morel & Garrigos (1982) have shown that S1 exists in the form of a rapid monomer–dimer equilibrium, the difference between the sedimentation coefficients of the monomer (5.05 S) and the dimer (6.05 S) (both at 20 °C) is rather low. These authors have taken great care in their sedimentation analyses, and it would be astonishing that the value of 5.05 S would be largely erroneous. However, the widely accepted value for the sedimentation coefficient of S1 at 20 °C is 5.80 S, although there is some discrepancy with the recent value of 6.00 S obtained by Mendelson & Kretzschmar (1980). The minimum value obtained by Lowey et al. (1969) is 5.70 S, and the maximum value obtained by Mendelson & Kretzschmar (1980) is 6.20 S. The difference between these extremes (0.50 S) is important and, to our minds, is due to the absence of controlled conditions for the sedimentation velocity analyses (see the introduction). Notwithstanding, owing to the scattering of the experimental data between 5.00 and 6.20 S, we shall consider, as an illustrating example, that the coefficient for the S1 monomer is 5.80 S at 20 °C (3.80 S at 4 °C), in order to have the inference of the choice for the exact value on the conclusions we have drawn above.

We have recomputed the long axis and the degree of hydration as in Tables III and IV, and we have observed that all the values of p ranging between 1.5 and 3.0 are compatible with the molecular weight and the three hydrodynamic data. Moreover, we have observed that the most probable values for the long axis and the degree of hydration, for $p = 2.3$, are respectively 155.5 Å and 1.33 g/g. These values are extremely close to those obtained with 5.05 S (156.5 Å and 1.37 g/g). Therefore, the model remains exactly the same for both values of s^0, in the limit of the experimental error.

Comments on Different Models for the S1 Monomer and the Myosin Heads. In their Figure 5, Mendelson & Kretzschmar (1980) compare the theoretical values of $I(h)$ with the experimental curve for various shapes of S1. They find very poor fits, even in the case of the pear shape found by Elliott & Offer (1978). As concerns the hydrodynamic properties of the pear-shaped molecule, Garcia de la Torre & Bloomfield
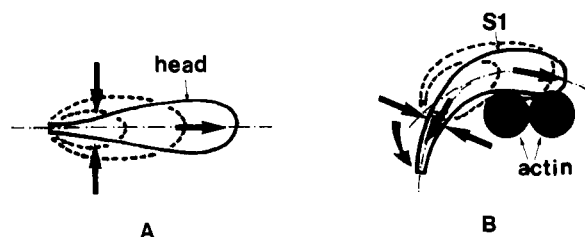
FIGURE 4: Schematic representation of the distortions occurring on dehydration, in the myosin head (A) and S1 bound to actin (B). The dashed lines represent the hollowed ellipsoid (hydrated). The arrows indicate the directions of the distortions. In both cases, the distortions can be mainly accounted for by a longitudinal stretching and a lateral shrinking (due to the removal of water from the hole). In case B, we have taken into account the fact that, in vitro, S1 is attached to two actin globules (Mornet et al., 1981). Note that a rotation of S1 occurs (curved arrow), leading to the comma-shaped molecule, attached to two actin globules belonging to two different strands (Amos et al., 1982).

(1980) have shown that, for the dehydrated molecule, $[\eta] \sim$ 2.6 cm^3/g and $s^0_{20,w} \sim 8.5$ S (with $M_r = 107\,000$ and $\bar{V} = V_{sp}$ = 0.673 mL/g). As concerns the value of θ^0, the problem is more complicated, but we can obtain an estimation of this parameter by replacing the protein by an equivalent ellipsoid with the same volume and the same long axis, since the long axis is the major parameter in this case (Tanford, 1967). This gives $p \sim 5$ and, by use of eq 19 and the calculations of Yang (1961) for J, $\theta^0 \sim 5.1 \times 10^5$ s^{-1}. By comparing these values with the experimental ones (Table I), we see that the fit is extremely poor. This clearly means that the head is highly hydrated. By increasing the degree of hydration (uniform expansion of the model), we get the best values for $\delta \sim 1.0$ g/g, which gives $[\eta] \sim 6.6$ cm^3/g, $s^0_{20,w} \sim 5.5$ S, and $\theta^0 \sim$ 2.1 $\times 10^5$ s^{-1}. The value of $[\eta]$ is suitable, but the value of $s^0_{20,w}$ is slightly too high and the value of θ^0 far too low. Thus, the pear-shaped molecule cannot simultaneously predict the three hydrodynamic data. Moreover, the dehydrated head has a calculated value of R_G (50 Å) that is considerably higher than the value of 33 Å found in solution for both LC2-free S1 and Mg·S1 (Mendelson, 1982). This too high value of R_G should be compared with the too high value of the maximum chord (190 Å), as compared with that found in solution (120 Å). For all these reasons, we consider that the pear shape of the myosin head does not correspond to the shape of S1 in solution. However, the presence of a hole at one extremity of our ellipsoid could explain the pear shape obtained on dehydration, provided one considers that (i) the hole is located near the junction with the tail and (ii) a longitudinal stretching of the head occurs on dehydration (Figure 4).

In their Figure 6, Mendelson & Kretzschmar (1980) compare the theoretical value of $I(h)$ with the experimental curve for the three-dimensional reconstruction of electron micrographs of S1-decorated actin paracrystals. The fit is better but significantly worse than that we have obtained for curve 4 in our Figure 3. However, Mendelson & Kretzschmar (1980) have not checked whether their model predicts the three hydrodynamic parameters. We have roughly estimated them by modeling dehydrated S1 as a prolate ellipsoid of major axis of 120 Å (maximum chord of the solid model) and volume of 120 000 Å^3 (see above). This gives $p \sim 2.8$ and $R_G \sim 30$ Å (against 31–32 Å for the solid model; Mendelson & Kretzschmar, 1980). The calculated value of R_G proves that our modeling will predict with a sufficient accuracy the hydrodynamic parameters. By taking $M_r = 107\,000$ and $\bar{V} = V_{sp}$ = 0.673 mL/g, we obtain, for the dehydrated S1, $[\eta] \sim 2.3$ cm^3/g, $s^0_{20,w} \sim 9.2$ S, and $\theta^0 \sim 16.7 \times 10^5$ s^{-1}. These values

remarkably deviate from the experimental values, as is the case for the pear. This means once more that S1 is highly hydrated. By increasing the degree of hydration (uniform expansion of the model), we get the best values for $\delta \sim 1.2$ g/g, which gives $[\eta] \sim 6.7$ cm^3/g, $s^0_{20,w} \sim 5.7$ S, and $\theta^0 \sim 6.3 \times 10^5$ s^{-1}. The values of $[\eta]$ and θ^0 are suitable, but the value of $s^0_{20,w}$ is significantly too high. Therefore, as is the case for the pear-shaped model, the model of Mendelson & Kretzschmar (1980) cannot simultaneously predict the three hydrodynamic data. However, it is better suited than the pear. This is not very surprising, since this model has a value of p (2.8), which is not quite different from the value we have obtained here (2.3). Obviously, in doing our calculations for the "rehydrated" pear and S1, we have uniformly expanded the model for the dehydrated proteins, since it is impossible to predict how water is bound to the protein. Such a procedure might not be valid, and the calculations made on the rehydrated models are to be considered only as illustrating examples. The only firm conclusions we can draw are that the dehydrated models do not at all predict the hydrodynamic data and that S1 and the myosin heads are extremely highly hydrated, which confirms our above calculations.

As a general comment, we have seen that, according to our approach, the S1 monomer in solution is extremely highly hydrated. As pointed out by Morel & Garrigos (1982), by use of eq 5 here, this conclusion is independent of the choice for the shape of S1. This is also confirmed by the above calculations, according to which the three hydrodynamic parameters, for both the dehydrated pear-shaped model and the dehydrated three-dimensional reconstructed model, are extremely different from those obtained in solution. Moreover, when these models are rehydrated, it is impossible to fit all the available data, and this means that distortions occur on dehydration. This is also the opinion of Yang & Wu (1977): "there is a certain risk by presuming that the shape of a protein molecule remains unaltered at all when the molecule is dried". We conclude that it is dangerous to compare data obtained in solution [R_G, $I(h)$, ...] with data obtained by means of conventional electron microscopy, for a so highly hydrated protein. It has been shown that the pear model does not predict the X-ray scattering data (Mendelson & Kretzschmar, 1980). Furthermore, we have shown here that it does not predict the hydrodynamic data. As concerns the three-dimensional reconstructed S1, the problem is much more complicated, since this model predicts reasonably well the X-ray scattering data. However, it does not predict the hydrodynamic data, but this conclusion might depend on the procedure used to account for bound water. Anyhow, we consider our hollowed ellipsoid is probably the best model for S1 in solution, since our calculations are all based on data obtained in solution only. Moreover, this model could provide explanations for the pear-shaped head (see above) and for the comma-shaped S1 attached to actin. Nevertheless, in this case attachment to actin would induce further distortions. In this context, we suggest that S1 attached to actin in vivo (hydrated state) might have the shape of a slightly distorted hollowed ellipsoid, more or less coiled round the actin filament (Figure 4).

Possible Variations in the Shape and/or Degree of Hydration of the S1 Monomer with Temperature. Let us assume that the hydrated S1 monomer keeps the shape of a prolate ellipsoid, irrespective of the temperature. By combining eq 1–3b and 16 and rearranging, we obtain

$$[\eta]_t/[\eta]_4 = (\nu_t/\nu_4)[(pb^3)_t/(pb^3)_4] \qquad (20)$$

$$(s^0_{t,w}\eta_t)/(s^0_{4,w}\eta_4) = (F_t/F_4)[(pb^3)_4/(pb^3)_t]^{1/3} \qquad (21)$$

$$[T/(\eta\theta^0)]_t/[T/(\eta\theta^0)]_4 = (J_4/J_t)[(pb^3)_t/(pb^3)_4] \quad (22)$$

The subscripts "4" and "t", respectively, refer to 4 and t °C. In these equations, we have neglected the variations of $\bar{V}$ with t. η is the viscosity of water. By combining eq 20 and 22 and eq 21 and 22, respectively, we get

$$[\eta]_t/[\eta]_4 = (\nu_t/\nu_4)(J_t/J_4)[[T/(\eta\theta^0)]_t/[T/(\eta\theta^0)]_4] \quad (23)$$

$$(s^0_{t,w}\eta_t)/(s^0_{4,w}\eta_4) =$$
$$(F_t/F_4)(J_4/J_t)^{1/3}[[T/(\eta\theta^0)]_4/[T/(\eta\theta^0)]_t]^{1/3} \quad (24)$$

Let us assume, as an illustrating example, that $t = 20$ °C. According to Table I, the mean value of θ^0_{20} is 8.16×10^5 s^{-1} and the most probable value of θ^0_4 is 6.54×10^5 s^{-1} (see above). Equations 23 and 24, therefore, give

$$[\eta]_{20}/[\eta]_4 = 1.33(\nu_t/\nu_4)(J_t/J_4) \quad (25)$$

$$(s^0_{t,w}\eta_t)/(s^0_{4,w}\eta_4) = 0.91(F_t/F_4)(J_4/J_t)^{1/3} \quad (26)$$

Under the assumption that the shape of the hydrated protein is independent of the temperature, the different shape factors are the same at 4 and 20 °C, and eq 25 and 26 reduce to

$$[\eta]_{20}/[\eta]_4 = 1.33 \quad (s^0_{20,w}\eta_{20})/(s^0_{4,w}\eta_4) = 0.91 \quad (27)$$

This means that different values for both $[\eta]$ and $s^0\eta$ should be observed at 4 and 20 °C, which is not the case, since Yang & Wu (1977) have found no significant difference in these parameters at 5 and 25 °C in the limit of the experimental error. Let us now assume that the value of p for the hydrated protein varies with t and that, for instance, p becomes 3.5 at 20 °C, instead of 2.3 at 1–5 °C. By making use of Table II, we now get

$$[\eta]_{20}/[\eta]_4 = 1.08 \quad (s^0_{20,w}\eta_{20})/(s^0_{4,w}\eta_4) = 1.00 \quad (28)$$

In this illustrating example we see that $s^0\eta$ is independent of t and that the variation in $[\eta]$ is of the order of magnitude of the incertitude at a given temperature (at 4 °C, 7.10/5.90 = 1.20; see Table I). We conclude that the value of p, for the hydrated S1 monomer, most likely increases by increasing t. It is interesting to see whether, in these conditions, the degree of hydration also varies. When it is always assumed that $\bar{V}$ is independent of t, eq 17 gives

$$[\eta]_{20}/[\eta]_4 = (\nu_{20}/\nu_4)[(\bar{V} + \delta_{20})/(\bar{V} + \delta_4)] = 1.08 \quad (29)$$

Now, according to Table II, we have $\nu_{20}/\nu_4 = 1.33$. By taking $\bar{V} = 0.739$ mL/g and $\delta_4 = 1.37$ g/g, we obtain $\delta_{20} = 0.97$ g/g, which means that the degree of hydration decreases with t. From this calculation, one might conclude that, when t increases, δ decreases. However, one must be extremely cautious with such a conclusion. In fact, we have oversimplified the problem by assuming the same value of p for the three ellipsoids (hydrated protein, dry protein, and hole). It is possible that these three ellipsoids have different values of p. Under such conditions, it remains clear that the value of p for the hydrated protein very likely increases with t (see above). However, it is difficult to know whether the value of p for the dry protein also increases. An interesting possibility to remove this ambiguity would be to do X-ray scattering observations [R_G, $I(h)$, ...], as those done by Mendelson & Kretzschmar (1980), at 20 °C, instead of 1 °C. Indeed, in this case only the dry protein is observed, and a variation in its shape would be detectable, if it exists. Note that Squire (1981) quotes a value of $R_G = 35$ Å, presumably at 20 °C (Table I). This feature is significantly higher than that found at 1–5 °C (33 Å; Table I) and is explainable on the basis of a higher value of p at 20 °C, for the dry protein (see eq 8).

Conclusion

By making use of a mathematical procedure deduced from that presented by Yang & Wu (1977), we were able to determine that S1 in solution can be modeled as a prolate ellipsoid of moderate axial ratio (between 1.0 and 2.5 at 4 °C). Calculations of the radius of gyration for ellipsoids with no hole indicate that the axial ratio is greater (between 3.0 and 3.5). However, for both 3.0 and 3.5, the discrepancy between the calculated and the measured values of the intensity of X-ray scattering is considerable. In sharp contrast, when a hole (filled with bound water) exists at one extremity of the protein, it is possible to fit both the values of the radius of gyration and the intensities of X-ray scattering. The best fit with the available experimental data (at 1–5 °C) is obtained for an axial ratio of 2.3 and a rather large hole, located at one extremity of the protein. Moreover, the degree of hydration is extremely high (more that 1 g/g), which is unusual for a protein. Our model would give a straightforward explanation for the pear shape of the myosin head, after dehydration. It also appears that dehydration induces other noticeable distortions. For instance, the maximum length of the dehydrated head is 190 Å (Elliott & Offer, 1978), while it is only ~120 Å in solution. Dehydration would, therefore, induce a stretching in the head. The difference between 190 and 120 Å cannot be accounted for by an important digestion during the preparation of S1. In fact, the molecular weight of total S1 (Mg·S1), recalculated in the present paper, ranges between 125 000 and 127 000. This gives a molecular weight for the whole myosin molecule of 2(125 000–127 000) + 220 000 = 470 000–474 000 [220 000 corresponds to the rod (Margossian et al., 1981)]. This value for the molecular weight of myosin is exactly the same as the most recent experimental value reported by Emes & Rowe (1979). This confirms that the amount of digested material is negligible. As far as it is possible to assume that the present study gives dimensions which are closer to the dimensions of the heads in vivo, than those obtained by Elliott & Offer (1978), the model of Offer & Elliott (1978) for the role of the two myosin heads might be now questionable. In fact, this model is mainly based on the shape and dimensions of dehydrated myosin heads. As concerns S1 attached to actin and observed by means of electron microscopy, the problem is also complicated, since S1 has neither the shape of a pear nor that of an ellipsoid. In this case, both dehydration and binding to actin lead to numerous distortions, as compared with S1 in solution.

Finally, we have found that the specific gravity of bound water is 0.956 g/mL, which confirms directly and for the first time the old hypothesis, according to which bound water has a structure quite different from that of bulk water. At first approximated, bound water might correspond, in the case of the S1 monomer, to a mixture of about 53% ice and 47% free water (at 4 °C).

In conclusion, the model we propose for the shape, dimensions, and degree of hydration of the S1 monomer in solution is able to describe quite well a number of different properties of this protein: intrinsic viscosity, sedimentaion coefficient, rotary diffusion coefficient, molecular weight, radius of gyration, volume, longest and most probable chords, and the complete X-ray scattering curve. As far as we know, no other model has been proved to be able to simultaneously describe all these properties.

Added in Proof

Sutoh (1983) has found that S1 in solution would be attached to only one actin globule, not to two as found by Mornet
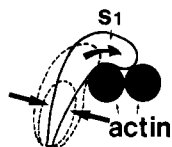
FIGURE 5.

et al. (1981). If the experimental finding of Sutoh is confirmed, Figure 4B in the main text should be replaced by Figure 5, which takes into account the fact that, on dehydration, S1 attaches to two actin globules (Amos et al., 1982).

Acknowledgments

We are extremely grateful to Dr. R. A. Mendelson for kindly furnishing to us the deconvoluted intensities of X-ray scattering and for his very helpful comments concerning bead modeling for scattering calculations. We are indebted to Professor J. T. Yang for helpful discussions and for furnishing to us his results concerning the intrinsic viscosities of S1(A1) and S1(A2).

References

Amos, L. A., Huxley, H. E., Holmes, K. C., Goody, R. S., & Taylor, K. A. (1982) *Nature (London)* 299, 467–469.
Elliott, A., & Offer, G. (1978) *J. Mol. Biol. 123*, 505–519.
Emes, C. H., & Rowe, A. J. (1979) *Biochim. Biophys. Acta 537*, 110–124.
Garcia Bernal, J., & Garcia de la Torre, J. (1980) *Biopolymers 19*, 751–766.
Garcia de la Torre, J., & Bloomfield, V. (1980) *Biochemistry 19*, 5118–5123.
Kobayashi, S., & Totsuka, T. (1975) *Biochim. Biophys. Acta 376*, 375–385.
Kretzschmar, K. M., Mendelson, R. A., & Morales, M. F. (1978) *Biochemistry 17*, 2314–2318.
Lowey, S., Slayter, H. S., Weeds, A. G., & Baker, H. (1969) *J. Mol. Biol. 42*, 1–29.
Margossian, S. S., & Stafford, W. F., III (1979) *Biophys. J. 25*, 20a.
Margossian, S. S., Stafford, W. F., III & Lowey, S. (1981) *Biochemistry 20*, 2151–2155.
Mendelson, R. A. (1982) *Nature (London) 298*, 665–667.
Mendelson, R. A., & Kretzschmar, K. M. (1980) *Biochemistry 19*, 4103–4108.
Mendelson, R. A., & Giniger, E. S. (1982) *Biophys. J. 37*, 54a.
Mendelson, R. A., Morales, M. F., & Botts, J. (1973) *Biochemistry 12*, 2250–2255.
Morel, J. E., & Garrigos, M. (1982) *Biochemistry 21*, 2679–2686.
Mornet, D., Bertrand, R., Pantel, P., Audemard, E., & Kassab, R. (1981) *Nature (London) 292*, 301–306.
Offer, G., & Elliott, A. (1978) *Nature (London) 271*, 325–329.
Parrish, R. G., & Mommaerts, W. F. H. M. (1954) *J. Biol. Chem. 209*, 901–913.
Sakura, J. O., & Reithel, F. J. (1972) *Methods Enzymol. 26*, 107–119.
Squire, J. M. (1981) in *Structural Basis of Muscular Contraction*, pp 240–244, Plenum Press, New York.
Sutoh, K. (1983) *Biochemistry 22*, 1579–1585.
Svedberg, T., & Pedersen, K. O. (1940) in *The Ultracentrifuge*, p 445, Oxford University Press, London.
Tanford, C. (1967) in *Physical Chemistry of Macromolecules*, Oxford University Press, London.
Thomas, D. D., Seidel, J. C., Hyde, J. S., & Gergely, J. (1975) *Proc. Natl. Acad. Sci. U.S.A. 72*, 1729–1733.
Tinoco, I., Jr., Sauer, K., & Wang, J. C. (1978) in *Physical Chemistry. Principles and Applications in Biological Sciences*, p 235, Prentice-Hall, Englewood Cliffs, NJ.
Yang, J. T. (1961) *Adv. Protein Chem. 16*, 323–400.
Yang, J. T., & Wu, C. C. (1977) *Biochemistry 16*, 5785–5789.

Formation of a Supramolecular Complex Is Involved in the Reconstitution of Basement Membrane Components[†]

Hynda K. Kleinman,* Mary L. McGarvey, John R. Hassell, and George R. Martin

ABSTRACT: Basement membrane macromolecules, including type IV collagen, laminin, and heparan sulfate proteoglycan, do not aggregate when incubated alone. Rather, precipitation occurs in the presence of equimolar amounts of laminin and type IV collagen but variable amounts of heparan sulfate proteoglycan. This interaction requires native laminin and type IV collagen. Heparan sulfate proteoglycan increases the precipitation of laminin particularly in the presence of type IV collagen. Fibronectin does not cause type IV collagen to precipitate. These studies show that the components of basement membrane interact in a highly specific manner and suggest that such interactions may be involved in the deposition of basement membrane in situ.

Basement membranes are thin extracellular matrices which support epithelial and endothelial cells and separate them from the underlying stroma. Progress has been made in defining the structure of basement membrane and its components (Kefalides, 1973; Heathcote & Grant, 1981; Timpl & Martin,

1982). All basement membranes contain type IV collagen (Kefalides, 1973; Yaoita et al., 1978; Timpl et al., 1978); laminin (Timpl et al., 1979; Chung et al., 1979; Foidart et al., 1980), and a heparan sulfate proteoglycan (Hassell et al., 1980) which are unique to basement membranes. Type IV collagen (M_r 540 000) is incorporated directly into the matrix without enzmatic processing to a less soluble form as observed with other collagen types (Minor et al., 1976; Heathcote et al., 1978; Dehm & Kefalides, 1978; Tryggvason et al., 1980;